Assessment of Meander-Line Antenna Covered with Dielectric Material for LHW Heating

Hiroki MATSUNO, Shuichi TAKAMURA, Shun HOSOI[1)] and Noriyasu OHNO[2)]

Department of Energy Engineering and Science, Nagoya University, Nagoya 464-8603, Japan
[1)]*Department of Electrical Engineering and Computer Science, Nagoya University, Nagoya 464-8603, Japan*
[2)]*EcoTopia Science Institute, Nagoya University, Nagoya 464-8603, Japan*

(Received 8 December 2005 / Accepted 19 January 2006)

A new analysis of meander-line type antenna with dielectric cover is presented and compared with experimental results. In the case of small research tokamaks for which the lower hybrid range of frequency is relatively low, a meander-line antenna with a strip-line structure would be preferable for LHW electron heating. When the antenna is installed in the vacuum chamber, it needs an insulating cover to protect it from plasma bombardment. The comparison between the analysis and experiments agree well if the thickness of the antenna conductor is sufficiently thin and there is no vacuum gap among the substrate, conductor, and cover. We found that a slow-wave antenna may be fabricated for LHW electron heating in the small tokamak HYBTOK-II under the driving frequency of, for example, 220 MHz.

Keywords: lower hybrid wave, meander-line antenna, slow-wave structure, small tokamak, electron heating

DOI: 10.1585/pfr.1.009

1. Introduction

Lower hybrid waves (LHW) have been employed for plasma current drive and electron heating in tokamak plasmas. For the accessibility of LHW into plasma it is necessary to have a large refractive index for the wave parallel to the static magnetic field, that is, a slow-wave structure. Furthermore, for heating electrons in plasmas, it is required that the phase velocity of the excited wave be smaller than several times of the electron thermal velocity. A phased waveguide array is used for wave excitation in medium size and large tokamaks [1]. However, in the case of small research tokamaks for which the electron temperature, the static toroidal magnetic field and the plasma density are not high, and then the lower hybrid range of frequency is relatively low, a meander-line antenna with a strip-line structure is preferable for a few tens of kilowatts of heating power [2–4]. A meander-line antenna consists of a microstrip meander conductor, and has a periodic structure in the direction of the toroidal magnetic field. It excites a traveling slow-wave if the absorption is sufficiently effective without any reflection at the antenna end. The refractive index of the excited wave parallel to the toroidal magnetic field depends on the microstrip line length perpendicular to the direction of traveling wave, the pitch length of the periodic structure, the thickness of the substrate and its dielectric constant. When the antenna is installed in the vacuum chamber, it needs an insulating cover to protect it from plasma bombardment. The dielectric constant and thickness of the cover may also change the antenna characteristics. In the past an experiment on a meander-line antenna was performed on a small size tokamak (T_e = 15 eV) for LHW heating and current drive [4], and tail electrons up to about 200 eV were observed.

The purposes of this work are, first of all, to develop new electromagnetic analysis on a meander-line antenna with a dielectric cover, and then to compare the new analysis and the experimental results. This enables us to estimate the properties of a covered antenna for lower hybrid wave heating. In addition, it provides a tool for estimating the dielectric constant of the insulating material used on an antenna, which is sometimes not known explicitly in this frequency range.

In the next section the analysis of a covered meander-line antenna is given. In Sec. 3, the experimental setup is introduced; the results of the experiment are shown in Sec. 4. Then we represent an application of the antenna in Sec. 5, and in Sec. 6 we provide a conclusion.

2. Analysis of Covered Meander-Line Antenna

The structure of the meander-line antenna is shown in Fig. 1. The microstrip meander conducting line with zero thickness for the numerical analysis is mounted on a dielectric substrate, which is sandwiched between a dielectric cover and grounded conductor. The line has turnbacks and then forms a periodic structure. A numerical analysis for such an antenna without an insulating cover has been performed [2]. A new electromagnetic analysis for the meander-line antenna with a dielectric cover is given in the

author's e-mail: h-matsuno@ees.nagoya-u.ac.jp

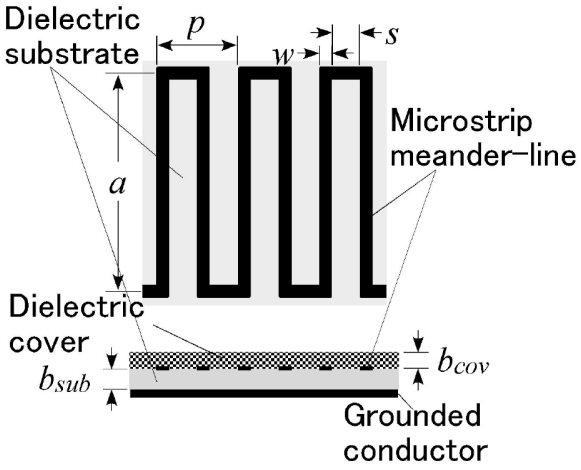

Fig. 1 Structure of the meander-line antenna, where a is the width of the meander structure, w the width of the microstrip line, s the spacing between two neighboring strip lines, p the pitch of the periodic structure, and $b_{\rm sub}$ and $b_{\rm cov}$ the thickness of the dielectric substrate and cover, respectively.

present paper. In the figure, a is the width of the meander structure, w the width of the microstrip line, s the spacing between two neighboring strip lines, p the pitch of the periodic structure, and $b_{\rm sub}$ and $b_{\rm cov}$ are the thickness of the dielectric substrate and cover, respectively. $K_{\rm sub}$ and $K_{\rm cov}$, the dielectric constants of the substrate and the cover, are also important parameters of the antenna. The objective is an assessment for actual employment of the type of antenna that would be used in small tokamaks. The antenna should be compatible with the possible plasma bombardment and have a substantially high $N_{//}$, which ensures the coupling of tail electrons in the plasma. It should be so compact that it may be installed in a rather small toroidal vacuum chamber.

First the Helmholtz equation is solved, and the potential and charge distribution on the microstrip line are obtained. A coordinate system for the numerical analysis is shown in Fig. 2. The equation is given by

$$\nabla^2\Phi + \left(\omega^2/c^2\right) K_{\rm eff}\Phi = 0, \tag{1}$$

where Φ is the electric potential, ω the angular frequency, c the speed of light, and $K_{\rm eff}$ the effective dielectric constant, which is determined later. The antenna structure is assumed to be uniform along the x-axis so that no turnbacks are considered at this stage. But we consider phase shifts along the conducting line under the quasi TEM approximation. Along the z-axis there is a periodicity (pitch p). Taking these into account, we get

$$\Phi(x,y,z) = U(y,z)\,\exp(\pm ikx), \tag{2}$$

$$U = \sum_{m=-\infty}^{+\infty} \{A_m \exp(\beta_m y) + B_m \exp(-\beta_m y)\} \exp(i\beta_m z), \tag{3}$$

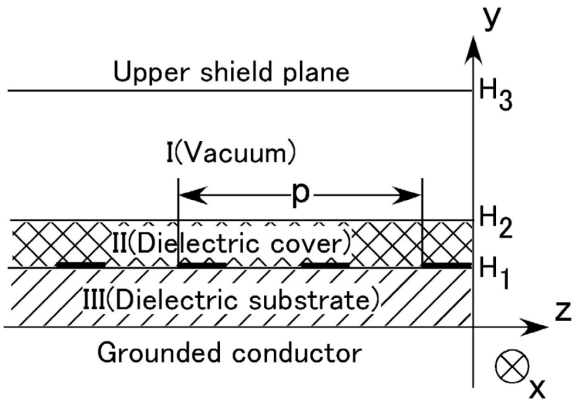

Fig. 2 Coordinate system for numerical analysis. Two dielectric layers are shown in the hatched regions. A cross section of microstrip lines is shown by horizontal thick lines in the interface.

where $k^2 = \omega^2 K_{\rm eff}/c^2$, $\beta_m = (\varphi + 2\pi m)/p$, φ is the phase shift on a unit cell of the meander-line, and i is the imaginary unit. Taking the boundary condition of $U = 0$ at $y = 0$ and H_3, the expression of U for each area $U_{\rm I}$, $U_{\rm II}$, $U_{\rm III}$ is given as follows:

$$\begin{cases} U_{\rm I} = \displaystyle\sum_m A_m e^{i\beta_m z} \sinh\{|\beta_m|(H_3 - y)\}, \\ U_{\rm II} = \displaystyle\sum_m \left(B_m e^{\beta_m y} + C_m e^{-\beta_m y}\right) e^{i\beta_m z}, \\ U_{\rm III} = \displaystyle\sum_m D_m e^{i\beta_m z} \sinh(|\beta_m| y). \end{cases} \tag{4}$$

Now, let the microstrip line be divided into N very narrow substrips, and let a substrip of width δ be centered at z' and furnished with a charge of uniform surface density. From the continuity condition at the boundaries $y = H_1$ and H_2, the coefficients $A_m \sim D_m$ are determined by the following equations:

$$\begin{cases} A_m = \sinh(|\beta_m|H_1)\Big[\sinh\{|\beta_m|(H_3-H_2)\}\sinh\{|\beta_m|(H_2-H_1)\} \\ \qquad + \dfrac{1}{K_{\rm II}}\cosh\{|\beta_m|(H_3-H_2)\}\sinh\{|\beta_m|(H_2-H_1)\}\Big]\Theta D_m, \\ B_m = \dfrac{1}{2}\Big[\sinh\{|\beta_m|(H_3-H_2)\} \\ \qquad - \dfrac{1}{K_{\rm II}}\cosh\{|\beta_m|(H_3-H_2)\}\Big] e^{-\beta_m H_2} A_m, \\ C_m = \dfrac{1}{2}\Big[\sinh\{|\beta_m|(H_3-H_2)\} \\ \qquad + \dfrac{1}{K_{\rm II}}\cosh\{|\beta_m|(H_3-H_2)\}\Big] e^{\beta_m H_2} A_m, \\ D_m = \dfrac{\lambda}{\varepsilon_0|\beta_m|p} e^{-i\beta_m z'} \\ \qquad \dfrac{\sin(\beta_m\delta/2)}{\beta_m\delta/2} \dfrac{1}{\sinh(|\beta_m|H_1)\{K_{\rm III}\coth(|\beta_m|H_1) + K_{\rm II}\Theta\}}, \end{cases} \tag{5}$$

where Θ is given by

$$\Theta = \frac{K_{\mathrm{II}} + \coth\{|\beta_m|(H_3 - H_2)\}\coth\{|\beta_m|(H_2 - H_1)\}}{K_{\mathrm{II}}\coth\{|\beta_m|(H_2 - H_1)\} + \coth\{|\beta_m|(H_3 - H_2)\}}. \tag{6}$$

Then, the potential at (y, z) when the charge λ on a substrip $(y = H_1, z = z')$ is given, corresponding to the Green function $g(y, z|H_1, z')$, is written by

$$g(y, z|H_1, z') = \sum_m \frac{\lambda}{\varepsilon_0|\beta_m|p} \mathrm{e}^{i\beta_m(z-z')} \frac{\sin(\beta_m\delta/2)}{\beta_m\delta/2} \frac{1}{K_{\mathrm{III}}\coth(|\beta_m|H_1) + K_{\mathrm{II}}\Theta}, \tag{7}$$

where K_{II} and K_{III} are the dielectric constants on the regions II and III shown in Fig. 2. The charge distribution on the line is given by solutions of the following equation:

$$\sum_{n=1}^{N} [\lambda_n g(H_1, z_n'|H_1, z_n) \pm \lambda_n^* g(H_1, z_n'|H_1, -z_n)] = \exp(i\varphi/4). \tag{8}$$

This is an $N \times N$ algebraic system of equations, and K_{eff} is given by

$$K_{\mathrm{eff}} = C_{\mathrm{K}}/C_1, \tag{9}$$

where C_{K} is the capacitance between the ground and the meander-line, calculated when K_{II} and K_{III} are the dielectric constants of the cover and the substrate, and C_1 is the value when $K_{\mathrm{II}} = K_{\mathrm{III}} = 1$. Considering the two strips in the unit cell, denoted by 1 and 2 for the left and right strip, respectively, we have the following voltages and currents:

$$\begin{aligned} v_1 &= [a_+ \exp(+ik_{\mathrm{e}}x) + a_- \exp(-ik_{\mathrm{e}}x) \\ &\quad - b_+ \exp(+ik_{\mathrm{o}}x) + b_- \exp(-ik_{\mathrm{o}}x)] \exp(-i\varphi/4), \\ v_2 &= [a_+ \exp(+ik_{\mathrm{e}}x) + a_- \exp(-ik_{\mathrm{e}}x) \\ &\quad + b_+ \exp(+ik_{\mathrm{o}}x) - b_- \exp(-ik_{\mathrm{o}}x)] \exp(+i\varphi/4), \end{aligned} \tag{10}$$

$$\begin{aligned} I_1 &= \{(1/Z_{\mathrm{e}})[a_+ \exp(+ik_{\mathrm{e}}x) - a_- \exp(-ik_{\mathrm{e}}x)] \\ &\quad + (1/Z_{\mathrm{o}})[-b_+ \exp(+ik_{\mathrm{o}}x) - b_- \exp(-ik_{\mathrm{o}}x)]\} \exp(-i\varphi/4), \\ I_2 &= \{(1/Z_{\mathrm{e}})[a_+ \exp(+ik_{\mathrm{e}}x) - a_- \exp(-ik_{\mathrm{e}}x)] \\ &\quad + (1/Z_{\mathrm{o}})[b_+ \exp(+ik_{\mathrm{o}}x) + b_- \exp(-ik_{\mathrm{o}}x)]\} \exp(-i\varphi/4), \end{aligned} \tag{11}$$

in which the coefficients $a_\pm$ and $b_\pm$ are the amplitudes of the even and odd modes, respectively, with propagation components in the $+x$ and $-x$ directions. Taking the length of the microstrip line along the x-axis a into account, the final dispersion relation of this antenna comes out under the condition of a turnback of the microstrip line,

$$\begin{aligned} &v_1\left(\frac{1}{2}a\right) = v_2\left(\frac{1}{2}a\right), \qquad I_1\left(\frac{1}{2}a\right) = -I_2\left(\frac{1}{2}a\right), \\ &v_2\left(-\frac{1}{2}a\right) = v_3\left(-\frac{1}{2}a\right), \quad I_2\left(-\frac{1}{2}a\right) = -I_3\left(-\frac{1}{2}a\right), \\ &v_3(x) = v_1(x)\exp(i\varphi), \qquad I_3(x) = I_1(x)\exp(i\varphi), \end{aligned} \tag{12}$$

$$\tan^2\frac{\varphi}{4} = \frac{Z_{\mathrm{o}}}{Z_{\mathrm{e}}} \begin{cases} \tan(k_{\mathrm{e}}a/2)\tan(k_{\mathrm{o}}a/2), \\ \cot(k_{\mathrm{e}}a/2)\cot(k_{\mathrm{o}}a/2). \end{cases} \tag{13}$$

The upper and lower equations are the dispersion relations for the forward and backward waves, respectively.

3. Experimental Setup

The antenna structure used in the test is shown in Fig. 3. The antenna parameters are as follows: $a = 83$ mm, $b_{\mathrm{sub}} = 3$ mm, $b_{\mathrm{cov}} = 3$ mm, $w = 2$ mm, $s = 3$ mm, $p = 2(w + s) = 10$ mm. It consists of the grounded conductor, the dielectric substrate, the microstrip meander-line, and the dielectric cover. The grounded conductor, the substrate, and the cover are fixed by screw bolts on the edge far from the antenna structure. Any thin separation in these plates was found to produce serious effects on the wave retardation. The grounded conductor is a stainless steel plate with a thickness of 2 mm. The substrate and the cover are also plates with a thickness of 3 mm. Three different kinds of materials (Teflon and two types of ceramics) were tested for these dielectrics. The antenna conductor is made of copper foil with a thickness of 0.01 mm (the skin depth of the copper is 3.8 μm on 300 MHz). Both ends of the antenna are terminated by a solid coaxial line.

The refractive index of the antenna is obtained from either the interference patterns or the phase of the picked-up electric field along the antenna, corresponding to $E_{//}$ along the direction of toroidal magnetic field, which may couple to the lower hybrid wave in tokamak plasmas. The measurement circuit is shown in Fig. 4. An RF signal (220 – 400 MHz, 10 dBm) is supplied to both the antenna and mixers. The other end of the antenna is terminated at 50 Ω through a solid coaxial line. The RF signal of the electric field at the antenna surface is received by a dipole pick-up antenna and transmitted to the balanced

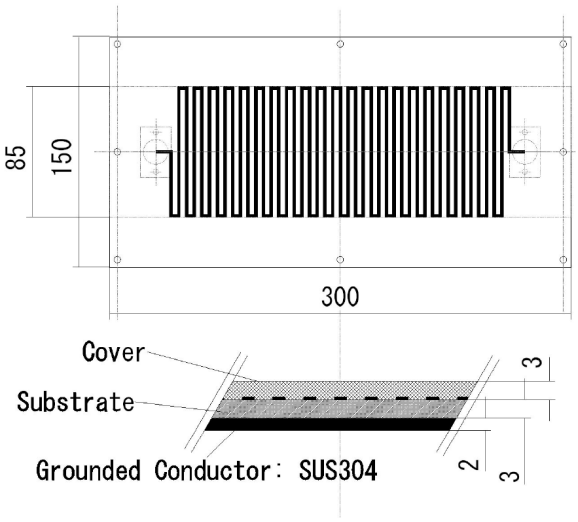

Fig. 3 Meander-line antenna for measurement. The numbers are in the unit of [mm].

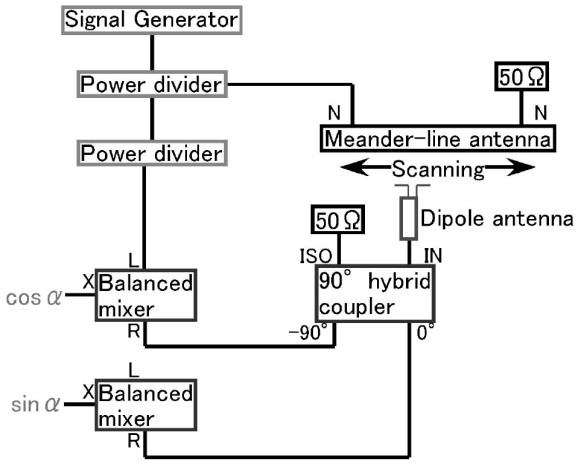

Fig. 4 Circuit for measurement of antenna characteristics. The electric field signal is scanned by the dipole antenna. Phase information is obtained by the output of the balanced mixers.

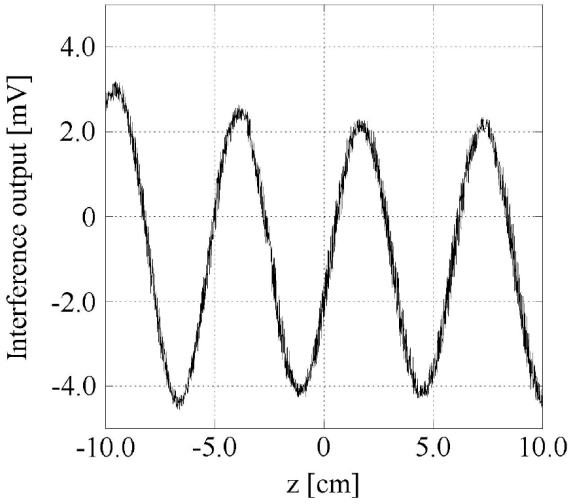

Fig. 5 A typical example of the interference pattern of the electric field along the meander-line antenna. The dielectric materials used as the substrate and the cover are Teflon. The frequency is 300 MHz.

mixer through a quadrature hybrid coupler. Then, we get a signal corresponding to the phase of the electric field from the mixer output. By scanning the dipole antenna along the z-axis, the field pattern is obtained. A typical interference pattern is shown in Fig. 5.

4. Experimental Results

The refractive indexes obtained in the experiment are plotted with discrete points in Figs. 6 and 7. The results of the numerical analysis are also shown by several kinds of curves in the same figures. Teflon and Shapal M Soft are used as the substrate in the cases of Figs. 6 and 7, respectively. The cases of four different cover materials (Teflon,

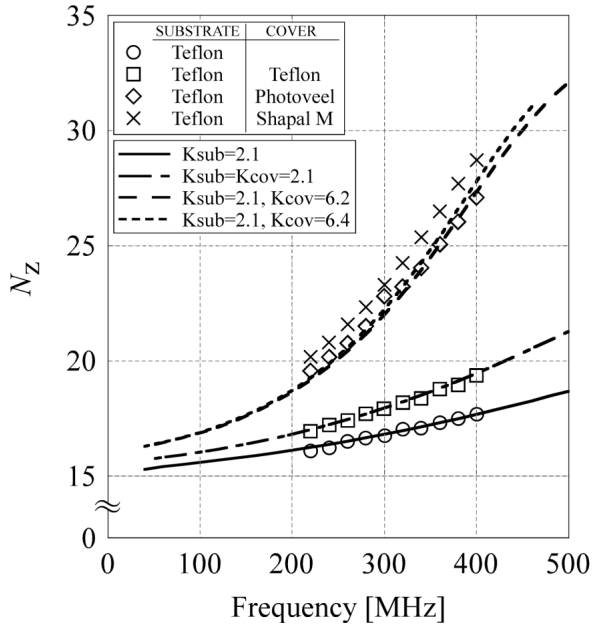

Fig. 6 Frequency dependence of N_z for the Teflon substrate. The N_z for four different combinations of the cover material (without cover, three dielectric materials) is plotted. The four curves are obtained by numerical analysis.

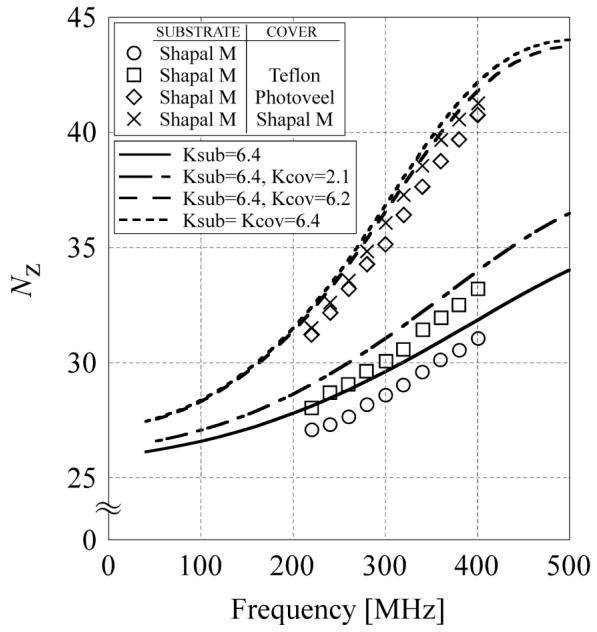

Fig. 7 Frequency dependence of N_z for Shapal M Soft substrate.

Shapal M Soft, Photoveel and without cover) are analyzed. Shapal M Soft and Photoveel are manufactured by MITSUI Mining Materials Co., Ltd, and SUMIKIN Ceramics & Quartz Co., Ltd, respectively. The length of the antenna used in the experiment is finite in the z-direction. Thus, the reflection of the wave at the edge of the meander-line structure may be envisaged. Since, in the experiment without plasma, the edge of the meander line is connected to

the signal generator, and the other is terminated by the 50 Ω terminator, we suppose that a small amount of reflection due to the deviation of the characteristic impedance of the microstrip line from 50 Ω would not create much disturbance, because the wave phase experimentally detected was found to be proportional to the distance along the antenna (z-direction). That is to say, it corresponds to the case of analysis where the antenna length is infinite in the z-direction.

Analyses well reproduce the experimental results when the dielectric constants are chosen as Teflon:2.1, Shapal M Soft:6.4, and Photoveel:6.2. The dielectric constants of these three materials at 1 MHz are Teflon:2.1, Shapal M Soft:7.0, Photoveel:6.0. Looking at the results of the Teflon, we can say that the analyses are consistent with the experimental results, since the dielectric constant of the Teflon doesn't depend so much on the frequency range employed. For the ceramics, the differences between the obtained dielectric constants and those at 1 MHz might indicate the existence of some frequency dependences.

We also found some surprising results for the thickness dependence of the microstrip conducting line, which is shown in Fig. 8. The antenna parameters are $a = 83$ mm, $b_{\mathrm{sub}} = 3.5$ mm, $w = 2$ mm, $s = 3$ mm, $p = 2(w + s) = 10$ mm, and is not covered. The open circles give experimental results for a microstrip line with a thickness of 2 mm. The retardation N_z for the antenna with a finitely thick conductor is substantially lower than the values estimated analytically without considering the thickness of the conductor, shown by the solid line in Fig. 8. The capacitance between two neighboring strip lines is significantly larger than that in the case of the numerical model, which would make the wave retardation weak; that is, the wave propagates in the z-direction rather than the x-direction.

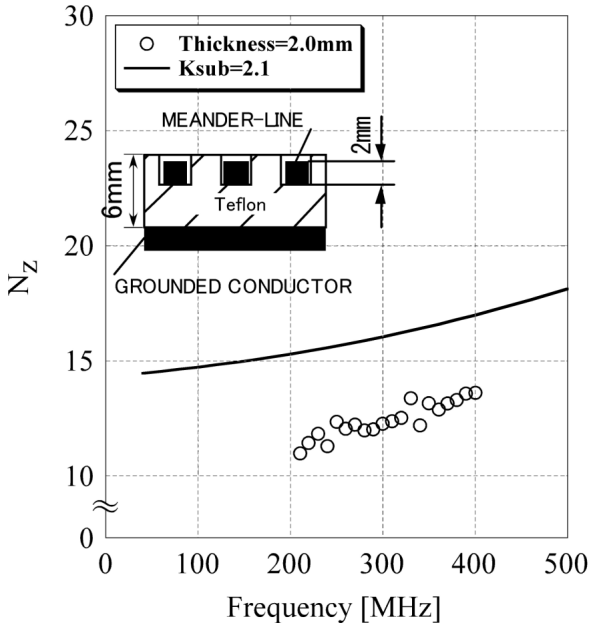

Fig. 8 Line thickness dependence on N_z. The meander-line conductor has a thickness of 2.0 mm. The substrate is made of Teflon, and has a meander-shape groove where the line is set.

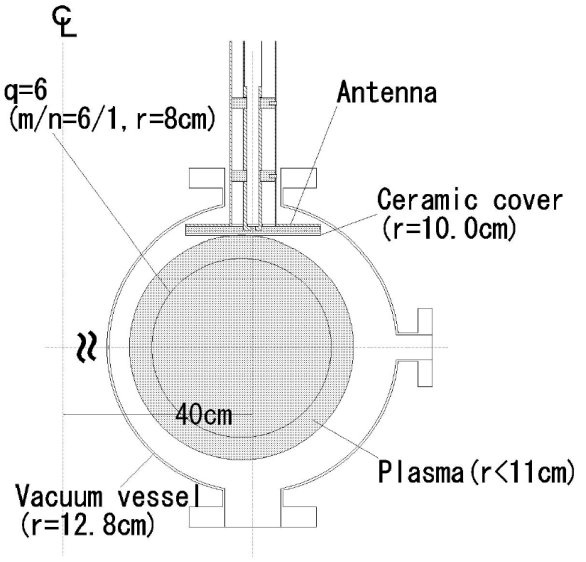

Fig. 9 Poloidal cross section of HYBTOK-II with the antenna and the plasma. The antenna is connected to a WX-39D coaxial tube. The plasma size may be regulated by the antenna. On typical operation the plasma horizontal position is 1 cm inside the poloidal center.

5. Fabrication of Slow-Wave Antenna for LHW Electron Heating

We are now trying to apply the meander-line antenna for electron heating by lower hybrid waves to the small tokamak device HYBTOK-II [5, 6]. The installation on the HYBTOK-II is shown as a poloidal cross section in Fig. 9. A picture of the antenna with a toroidal curvature is shown in Fig. 10. The driving frequency is 220 MHz. To protect the meander line from the plasma bombardment, a boron nitride plate is used as a cover. Since the cover separates the meander-line conductor from the tokamak plasma, it may ensure the excitation of the slow wave without any possible serious modification of the electric field structure near the microstrip line. The cover makes the coupling to the plasma weak when the thickness of cover is substantially large. We can adjust the antenna length and the cover thickness such that a traveling wave on the microstrip-line antenna attenuates almost entirely when the wave arrives at the antenna end. So it is thought that the antenna excites a slow wave in the plasma such as that given in the analytical and the experimental results in the previous sections. The size of the antenna needs to be as large as possible to have good power absorption and a sufficient parallel refractive index, which is thought to be $N_z = 22 \sim 38$ corresponding to the phase velocity of $3v_{\mathrm{te}} \sim 5v_{\mathrm{te}}$, $v_{\mathrm{te}} = (2kT_{\mathrm{e}}/m_{\mathrm{e}})^{1/2}$, considering the electron

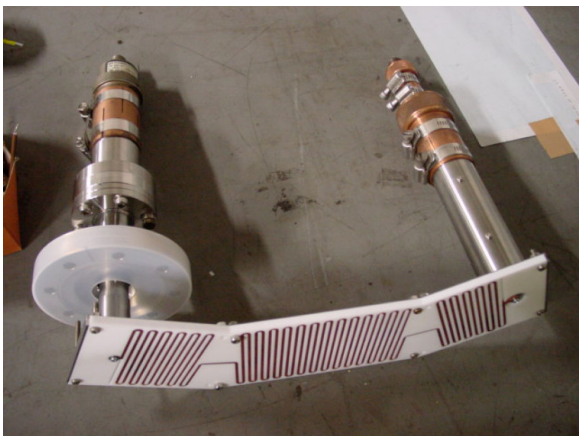

Fig. 10 The antenna to be installed in HYBTOK-II. The antenna without cover shows the meander-line conductor. The RF injection points of the antenna conductor are connected to the WX-39D, and the end to the WX-20D coaxial tube.

temperature of $T_e \approx 20\,\mathrm{eV}$. The strength of the coupling between the antenna and the plasma can be changed by proper selection of the cover thickness. A thick antenna makes for weaker coupling.

6. Conclusion

Numerical analysis and measurements of the refraction index of a microstrip meander-line type antenna are presented. Both are in good agreement if the thickness of the antenna conductor is sufficiently thin and there is no vacuum gap among the substrate, conductor, and cover. We found that a slow-wave antenna may be fabricated for LHW electron heating in the small tokamak HYBTOK-II under the driving frequency of 220 MHz. Tail electron heating would be expected at the electron temperature of around 20 eV. Comparing N_z between the experiment and the analysis enables us to determine the dielectric constant in this range of frequency. The dielectric cover was found to increase the refractive index of the antenna and to be useful for proper coupling.

Acknowledgments

The authors would like to thank Dr. S. Kajita for his valuable comments, and also to acknowledge Grant-in-Aid for Scientific Research on Priority Areas, No. 11210206.

[1] B.J. Ding, G.L. Kuang, J.F. Shan, G.S. Xu, M. Song *et al.*, Plasma Phys. Control. Fusion **46**, 1467 (2004).
[2] Jerald A.Weiss, IEEE Trans. Microwave Theory and Techniques MTT-22 **12**, 1194 (1974).
[3] T. Takahashi, S. Takamura and T. Okuda, J. Appl. Phys. **53**, 6693 (1982).
[4] K. Ushikusa, S. Takamura and T. Okuda, Nucl. Fusion **24**, 751 (1984).
[5] Y. Kikuchi, Y. Uesugi, S. Takamura and A.G. Elfimov, Nucl. Fusion **44**, S28 (2004) .
[6] S. Takamura, Y. Kikuchi, Y. Uesugi and M. Kobayashi, Nucl. Fusion **43**, 393 (2003).